

Estimating subglacial water geometry using radar bed echo specularity: application to Thwaites Glacier, West Antarctica

Dustin M. Schroeder, *Graduate Student Member, IEEE*, Donald D. Blankenship, R. Keith Raney, *Life Fellow, IEEE*, Cyril Grima

Abstract—Airborne radar sounding is an established tool for observing the bed conditions and subglacial hydrology of ice sheets and glaciers. The specularity content of radar bed echoes has also been used to detect the hydrologic transition of a subglacial water system from a network of distributed canals to a network of concentrated channels beneath Thwaites Glacier. However the physical dimensions of the distributed water bodies in these networks have not been constrained by observations. In this paper, we use a variety of simple radar scattering, attenuation, and cross section models to provide a first estimate of the subglacial water body geometries capable of producing the observed anisotropic specularity of the Thwaites Glacier catchment. This approach leads to estimates of ice/water interface rms roughnesses less than about 15 cm, thicknesses of more than about 5 cm, lengths of more than about 15 m, and widths between about 0.5 and 5 m.

Index Terms—subglacial hydrology, ice penetrating radar, radar sounding, scattering function

I. INTRODUCTION

SOUNDING ice sheets with airborne ice penetrating radar is a powerful and well established tool for probing the interior structures and bed configuration of glaciers and ice sheets [1]–[6]. Glaciological and geophysical interpretations of ice penetrating radar records have advanced the observation and understanding of subglacial lakes and hydrologic systems [7]–[11]. These water systems can exert critical control on the behavior, evolution, and stability of marine ice sheets and their sea level contribution [12]–[14].

Traditional interpretation methods [8], [15]–[18], which rely on identifying subglacial water bodies as flat and bright interfaces in radargrams, are susceptible to erroneous interpretation due to uncertainty in englacial attenuation from observationally underconstrained ice temperature and chemistry [19]–[21]. To address this challenge, the specularity content of radar bed echoes (a parameterization of the along-track scattering function expressed in its Doppler distribution [22], [23]) has been used to provide an attenuation-independent proxy for distributed subglacial water bodies [11]. These water bodies are in hydrostatic equilibrium with the overlying ice and melt-freeze processes produce ice-water interfaces that are flat at

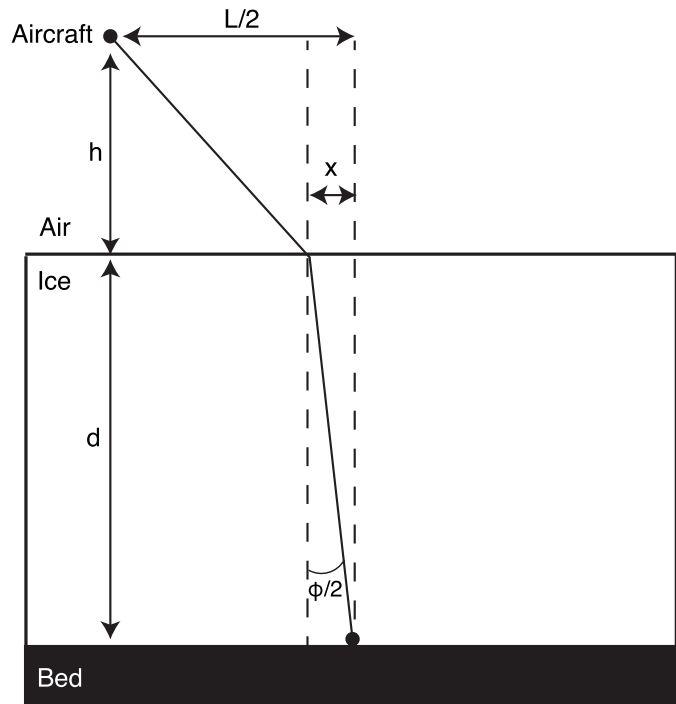


Fig. 1. Geometry for the path of a radar return from a point on the ice/bed interface

the wavelength scale [9], resulting in specular radar reflection [11].

The anisotropic specularity of radar bed echoes has been used to detect a subglacial water system beneath the upstream region of Thwaites Glacier composed of a network of distributed canals [14] eroded into the subglacial sediment [11]. Although their detection represents an unprecedented observation of the dynamically critical hydrologic state [12]–[14], [24] of subglacial water beneath a contemporary ice sheet, the geometry of the water bodies that make up these distributed networks have not been constrained by geophysical observation or analysis. In fact, the only prior use of radar sounding data to directly constrain the geometries of subglacial water bodies have been applied in East Antarctica [17] and Greenland [9], which have fundamentally different topographic, lithologic, and geothermal basal boundary conditions from Thwaites Glacier [25]–[29] in particular and West

Manuscript received XXXX X, 2014. D.M. Schroeder, D.D. Blankenship, and C. Grima are with the Institute for Geophysics, University of Texas, Austin, TX 78758 USA (e-mail: dustin.m.schroeder@utexas.edu; blank@ig.utexas.edu, cgrima@ig.utexas.edu). R.K. Raney resides in Annapolis, MD 21401 USA (e-mail: k.raney@ieee.org).

Digital Object Identifier: 10.1109/LGRS.2016.2337878

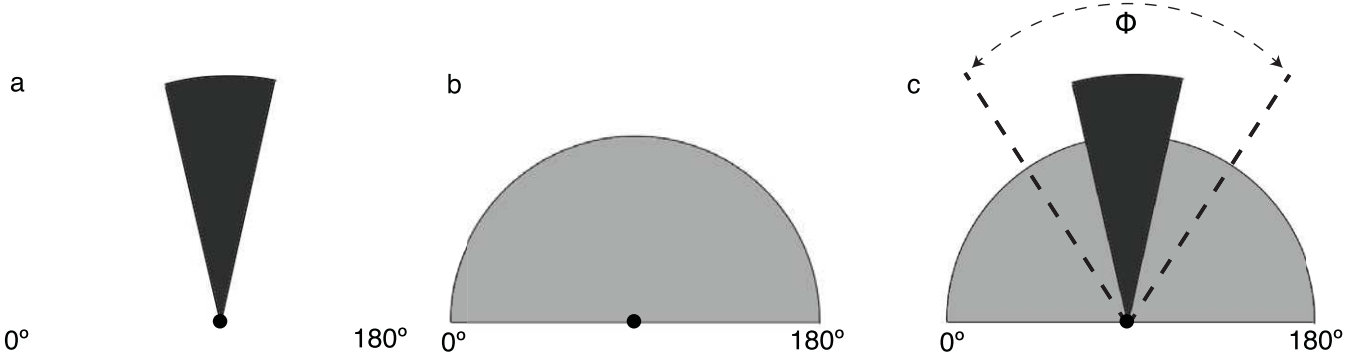


Fig. 2. Model for the scattering function of a) a purely specular reflecting interface, b) a purely diffuse isotropically scattering interface and c) an interface that returns both diffuse and specular energy.

Antarctica in general and, as such, support different regimes and configuration of subglacial water.

This paper aims to provide estimates of physical properties that can be inferred for subglacial water systems that produce anisotropic specular bed echoes. These estimates are useful for understanding and predicting the behavior of subglacial water systems, their control on ice sheet evolution, and their comparison to the geologic, morphologic, and sedimentary record of the subglacial water systems of paleo ice sheets.

II. SPECULARITY CONTENT OF BED ECHOES

SAR focusing [10], [30]–[35] of coherent radar sounding [36]–[41] data is achieved by convolving the recorded data with a reference function for the phase history of a point scatterer at the bed. The propagation path between an airborne radar and a point on the ice-bed interface is shown in Figure 1 and given by Snell's Law,

$$\frac{\frac{L}{2} - x}{\sqrt{h^2 + (\frac{L}{2} - x)^2}} = \frac{x\sqrt{\epsilon_r}}{\sqrt{d^2 + x^2}} \quad (1)$$

where L is the focusing reference aperture, h is survey height above the ice surface, d is the ice thickness, x is the displacement of the refraction point on the ice surface, and $\sqrt{\epsilon_r}$ is the index of refraction of ice [10], [33]. The specularity content of a bed echo [11] is a parameterization that models the along-track angular distribution of bed echo energy as an angularly narrow specular energy component S (Figure 2a) and an isotropic diffuse energy component D (Figure 2b) with the specularity content S_c of the bed echo given by

$$S_c = \frac{S}{S + D} \quad (2)$$

This value is calculated by focusing with two different apertures L_1 and L_2 [10]. In this case, the angles spanned by each are Φ_1 and Φ_2 (Figure 2c) given by

$$\Phi = 2 \tan^{-1}(x/d). \quad (3)$$

The energy focused by each is E_1 and E_2 and are given by

$$E_1 = S + D \frac{\Phi_1}{180^\circ} \quad (4)$$

and

$$E_2 = S + D \frac{\Phi_2}{180^\circ}, \quad (5)$$

so that the specularity content is

$$S_c = \frac{\frac{E_2}{E_2 - E_1} - \frac{\Phi_2}{180^\circ - \Phi_1}}{\frac{E_2}{E_2 - E_1} + \frac{180^\circ - \Phi_2}{\Phi_2 - \Phi_1}}. \quad (6)$$

Because both energies are focused through the same ice column, the englacial attenuation rate will be the same for both focused energies so that

$$E_1 = \left(S + D \frac{\Phi_1}{180^\circ} \right) 10^{ld_1/10} \quad (7)$$

and

$$E_2 = \left(S + D \frac{\Phi_2}{180^\circ} \right) 10^{ld_2/10}, \quad (8)$$

where l is the englacial attenuation rate and d_1 and d_2 are the mean ice thicknesses through which the bed echo energy focused by each aperture propagates. If we assume that $d_1 \approx d_2$, then equations 6, 7, and 8 show that the calculated specularity is unchanged. In practice, $d_1 = d_2$ for purely specular bed echoes and the difference between d_1 and d_2 results in an error of less than 0.2% for a highly diffuse bed with $h = 750$ m, $d = 2$ km, $L_1 = 700$ m, $L_2 = 2$ km, and $l = 10$ dB/km (typical values for the Thwaites Glacier [21], [25]). Therefore, the specularity content of radar bed echoes is a measure of the angular spread of the along-track scattering function that is highly insensitive to attenuation through the ice column.

III. ROUGHNESS OF THE ICE WATER INTERFACE

The specularity of a radar bed echo is determined, in part, by the roughness of the ice/water interface [42] (Figure 3). Under Kirchhoff assumptions, the unfocused echo energy returned at nadir E_0 is a function of the rms height of the reflecting interface (here assumed to be water) RMS_w and is given by

$$E_0 = e^{-g^2} I_0^2 (g^2/2), \quad (9)$$

where

$$g = 4\pi \text{RMS}_w f_c \sqrt{\epsilon_r}/c, \quad (10)$$

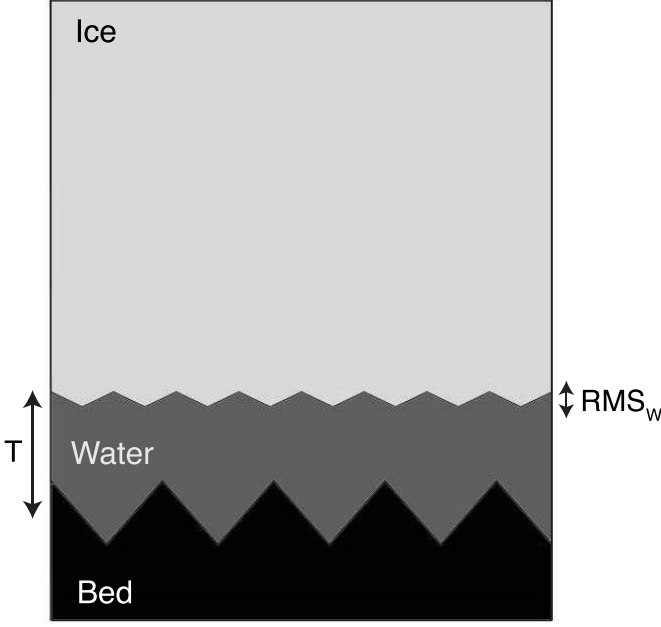


Fig. 3. Cartoon of the roughness of the ice-water interface RMS_w of a subglacial water layer of finite thickness T .

and f_c is the central frequency of the radar, c is the speed of light in a vacuum, and I_0 is the modified zeroth order Bessel function of the first kind [41]. Alternatively, the scattering function of surfaces that satisfy Kirchhoff assumptions can be modeled as a normal distribution of energy across scattering angles [43]. Since the energy is distributed normally, the unfocused echo energy returned at nadir can be calculated using an error function (erf) [42], given by

$$E_0 = \text{erf}\left(\frac{1}{2g}\right)_a \text{erf}\left(\frac{1}{2g}\right)_x \quad (11)$$

where erf_a models scattering in the along-track direction and erf_x models scattering in the across-track direction. Empirically, Equation 11 provides an approximation for Equation 9 (Figure 4). Notably, this approximation allows along-track focusing with different apertures to be easily modeled by changing the argument in the first error function (corresponding to scattering in the along-track direction).

$$E_i = \text{erf}\left(\frac{\Phi_i/\phi_F}{2g}\right) \text{erf}\left(\frac{1}{2g}\right), \quad (12)$$

where Φ_i is the range of scattering angles spanned by the focusing reference aperture and ϕ_F is the range of scattering angles spanned by the diameter of the 1st Fresnel zone D_1 at the bed (corresponding to the range of scattering angles in the unfocused nadir return), given by

$$\phi_F = 2 \tan^{-1}(D_1/2d) \quad (13)$$

and

$$D_1 \approx \sqrt{2c/f_c \left(h + \frac{d}{\sqrt{\epsilon_r}} \right)}. \quad (14)$$

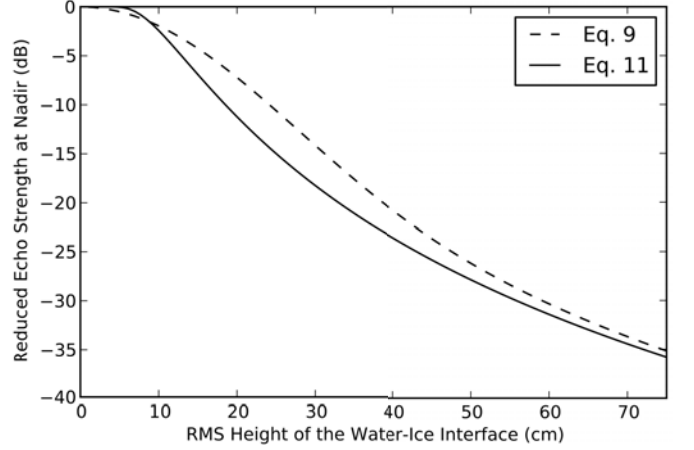


Fig. 4. Reduction in reflectance power at nadir as a function of surface roughness described by Equation 9 (dashed-line) and Equation 11 (solid line).

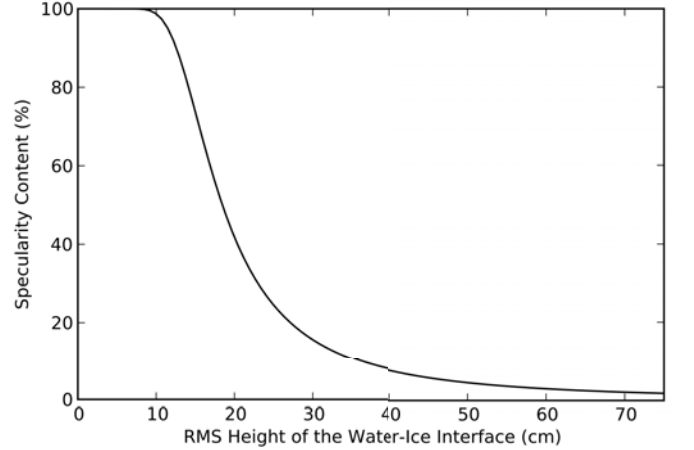


Fig. 5. Specularity of radar bed echoes as a function of the roughness of the ice-water interface.

With this model, the focused energies for each aperture are given by

$$E_1 = \text{erf}\left(\frac{\Phi_1/\phi_F}{2g}\right) \text{erf}\left(\frac{1}{2g}\right) \quad (15)$$

and

$$E_2 = \text{erf}\left(\frac{\Phi_2/\phi_F}{2g}\right) \text{erf}\left(\frac{1}{2g}\right) \quad (16)$$

and the specular content is given by Equation 6. Figure 5 shows that, for a survey height of $h = 750$ m, an ice thickness of $d = 2$ km, and focusing apertures of $L_1 = 700$ m and $L_2 = 2$ km (typical values for the Thwaites Glacier survey [11], [25]) high specularity values indicate an ice/water interface with rms heights less than about 15 cm.

IV. THICKNESS OF THE SUBGLACIAL WATER LAYER

In order to estimate the minimum thickness T of a specularly reflecting water layer, we model the bed echo energy of the ice/water interface as purely specular and the bed echo energy of the water/bed interface as purely diffuse (the

most pathological case for producing specular returns). We assume that the reflection coefficient for the ice/water R_w and water/bed R_b interfaces are determined by the real permittivity of the ice ϵ_i , water ϵ_w , and bed ϵ_b [41] and given by

$$R_w = \left| \frac{\sqrt{\epsilon_w} - \sqrt{\epsilon_i}}{\sqrt{\epsilon_w} + \sqrt{\epsilon_i}} \right| \quad (17)$$

and

$$R_b = \left| \frac{\sqrt{\epsilon_b} - \sqrt{\epsilon_w}}{\sqrt{\epsilon_b} + \sqrt{\epsilon_w}} \right| \quad (18)$$

We also assume that the specular component of the total bed echo energy is proportional to the reflection coefficient for the ice/water interface and increases exponentially with the fraction of the skin-depth (δ) occupied by the water layer thickness (T) (such that $S = 0$ for $T = 0$, S asymptotically approaches proportionality to R_w as T approaches ∞ , and S is reduced by e^{-1} at $T = \delta$ [17]), given by

$$S \propto R_w (1 - e^{-T/\delta}), \quad (19)$$

and

$$\delta = \sqrt{\frac{1}{\pi f_c \sigma_w \mu_0}}, \quad (20)$$

where σ_w is the conductivity of the water and μ_0 is the permittivity of free space. We assume that the diffuse bed return is attenuated by the two-way path through the water layer and is proportional to

$$D \propto R_b e^{-2T/\delta} \quad (21)$$

and the specular content of the total bed echo is given by Equation 2. Figure 6 shows that the depth of water required to produce specular returns is highly dependent on the conductivity σ_w of the subglacial water (and therefore its salinity and local geochemistry). Figure 6 also shows that (for $\epsilon_i = 3.17$, $\epsilon_w = 80$, $\epsilon_b = 18$, and $\sigma_w = 1$, which is typical of ground water [17], [41], [44]) specular water layers are expected to have thicknesses greater than about 5 cm.

V. LENGTH OF SUBGLACIAL WATER BODIES

Because the water system in the upstream portion of the Thwaites catchment is a network of distributed canals, we can approximate the reflecting geometry of its ice/water interface a rectangular plate (Figure 7) with radar cross section RCS [45] proportional to

$$RCS \propto \frac{\sin^2(k L_w \sin \phi)}{k^2 L_w^2 \sin^2 \phi} \quad (22)$$

for

$$\Theta = 0 \quad (23)$$

where Θ is the observation angle (the angle between the direction of water flow and the survey line), ϕ is the along-track scattering angle, k is the wavenumber, given by

$$k = 2\pi f_c / c \quad (24)$$

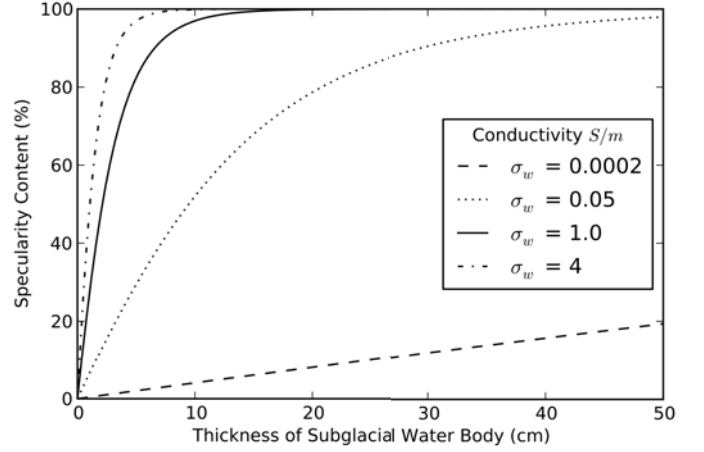


Fig. 6. Specularity content of radar bed echoes as a function of water layer thickness T and conductivity σ_w . (a σ_w value of about 0.0002 is typical of pure water, of about 4 is typical of sea water, and about 1 is typical of ground water [17], [41], [44])

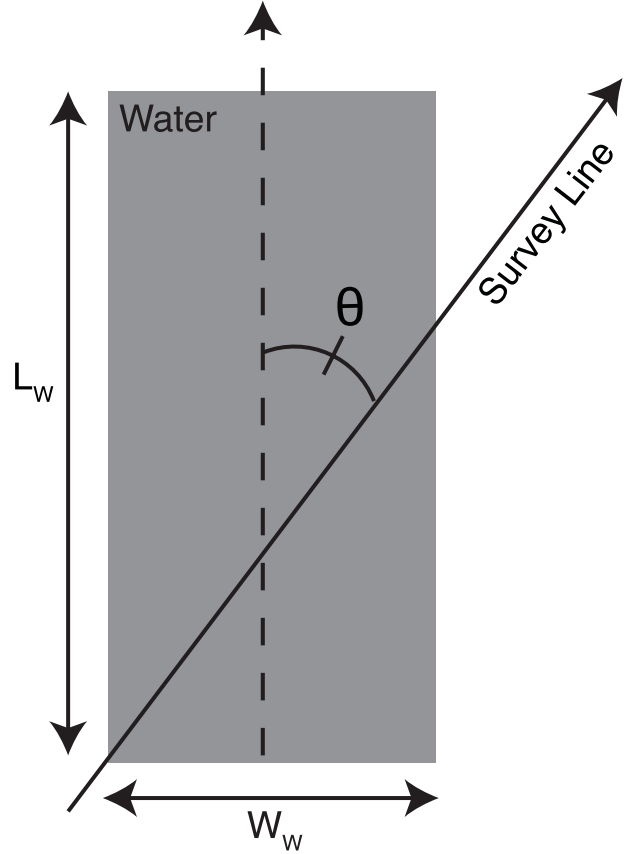


Fig. 7. Observation geometry for a subglacial water body with a rectangular reflecting interface.

and L_w is the length of the subglacial water body. In this case where $\Theta = 0$, the effect of subglacial water body width L_w on RCS can be assumed to be constant.

In order to estimate the effect of water body length on bed echo specularity, we calculate the focused echo energies E_1 and E_2 by integrating the radar cross section across the

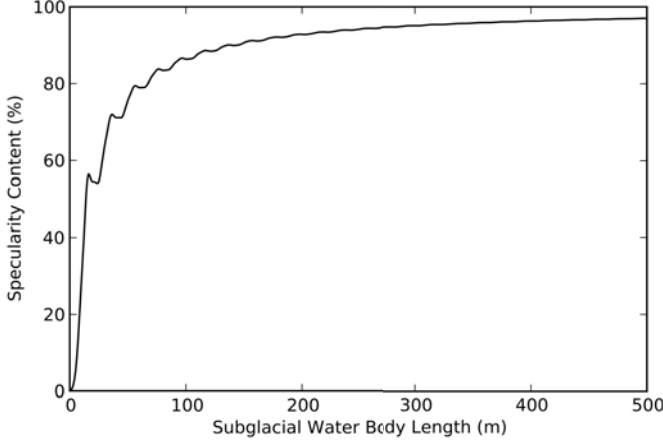


Fig. 8. Specularity content of radar bed echoes as a function of subglacial water body length

range of scattering angles $\pm\Phi_1/2$ and $\pm\Phi_2/2$ spanned by the focusing apertures and given by

$$E_1 = \int_{-\Phi_1/2}^{\Phi_1/2} \frac{\sin^2(kL_w \sin \phi)}{k^2 L_w^2 \sin^2 \phi} \delta\phi \quad (25)$$

$$E_2 = \int_{-\Phi_2/2}^{\Phi_2/2} \frac{\sin^2(kL_w \sin \phi)}{k^2 L_w^2 \sin^2 \phi} \delta\phi \quad (26)$$

Figure 8 shows that specular subglacial water bodies are detectable for lengths greater than about 15 meters.

VI. WIDTH OF SUBGLACIAL WATER BODIES

The distributed subglacial water systems observed beneath the upstream region of the Thwaites Glacier catchment are anisotropic [11] and produce bed echoes with specularity that varies as a function of observation angle. The rectangular plate model (Figure 7) for the radar cross section of a subglacial water body also varies as a function observation angle Θ and width W_w so that effective along-track length L_Θ is given by

$$L_\Theta = \begin{cases} \left| \frac{W_w}{\sin \Theta} \right|, & \text{for } \Theta > \tan^{-1}(W_w/L_w) \\ \left| \frac{L_w}{\cos \Theta} \right|, & \text{for } \Theta \leq \tan^{-1}(W_w/L_w) \end{cases} \quad (27)$$

and the focused echo energies are given by

$$E_1 = \int_{-\Phi_1/2}^{\Phi_1/2} \frac{\sin^2(kL_\Theta \sin \phi)}{k^2 L_w^2 \sin^2 \phi} \delta\phi, \quad (28)$$

and

$$E_2 = \int_{-\Phi_2/2}^{\Phi_2/2} \frac{\sin^2(kL_\Theta \sin \phi)}{k^2 L_w^2 \sin^2 \phi} \delta\phi \quad (29)$$

and the specularity content is given by Equation 6. Figure 9 shows that (for a length $L_w = 300$ m) subglacial water bodies that appear specular within about 30° of ice fl w and diffuse in the other can be estimated to have widths between about 50 cm and about 5 m.

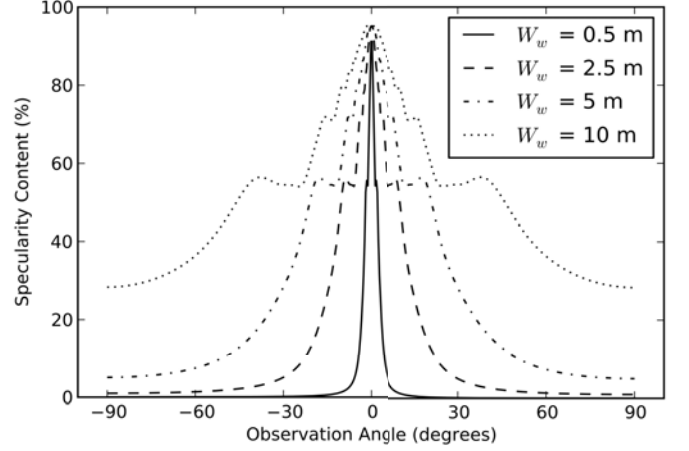


Fig. 9. Specularity content of radar bed echoes as a function of observation angle Θ_w and water body width W_w

VII. CONCLUSION

Although the scattering function and specularity of bed echoes of subglacial water result from a combination of these effects, our results provide an initial estimate of the physical dimensions of subglacial water bodies that can be inferred from the anisotropic specularity of bed echoes. We estimate that the subglacial water bodies in the upstream region of Thwaites Glacier, West Antarctica have ice/water interfaces with rms roughnesses less than about 15 cm, depths of more than about 5 cm, lengths from about 15 m to more than 75 m, and widths of between about 50 cm and 5 m.

ACKNOWLEDGMENT

We thank National Science Foundation (grant numbers PLR-0636724 and PLR-0941678), the National Aeronautics and Space Administration (grant number NNX08AN68G), and the G. Unger Vetlesen Foundation for supporting this work. DMS received support from a NSF GRFP Fellowship, a University of Texas Recruiting Fellowship, and the UTIG Gale White Fellowship. This is UTIG contribution XXXX.

REFERENCES

- [1] B. Steenson, C. I. of Technology. Division of Engineering, and A. Science, *Radar Methods for the Exploration of Glaciers*, ser. CIT theses. California Institute of Technology, 1951.
- [2] S. Evans and G. d. Q. Robin, "Glacier depth-sounding from the air," *Nature*, 1966.
- [3] S. Evans and B. Smith, "A radio echo equipment for depth sounding in polar ice sheets," *Journal of Physics E: Scientific Instruments*, vol. 2, no. 2, p. 131, 1969.
- [4] P. Gudmandsen, "Electromagnetic probing of ice," in *Electromagnetic probing in geophysics*, vol. 1, 1971, p. 321.
- [5] G. Oswald, "Investigation of sub-ice bedrock characteristics by radio-echo sounding," *Journal of Glaciology*, vol. 5, no. 73, p. 975, 1975.
- [6] D. J. Drewry, "Comparison of electromagnetic and seismic-gravity ice thickness measurements in east antarctica," *Journal of Glaciology*, vol. 15, pp. 137–150, 1975.
- [7] S. P. Carter, D. D. Blankenship, D. A. Young, and J. W. Holt, "Using radar-sounding data to identify the distribution and sources of subglacial water: application to Dome C, East Antarctica," *Journal of Glaciology*, vol. 55, no. 194, pp. 1025–1040, 2009.
- [8] G. K. A. Oswald and G. Robin, "Lakes Beneath the Antarctic Ice Sheet," *Nature*, vol. 245, no. 5423, pp. 251–254, Oct. 1973. [Online]. Available: <http://dx.doi.org/10.1038/245251a0>

- [9] G. K. A. Oswald and S. Gogineni, "Recovery of subglacial water extent from Greenland radar survey data," *Journal of Glaciology*, vol. 54, no. 184, pp. 94–106, 2008.
- [10] M. E. Peters, D. D. Blankenship, S. P. Carter, S. D. Kempf, D. A. Young, and J. W. Holt, "Along-Track Focusing of Airborne Radar Sounding Data From West Antarctica for Improving Basal Reflectio Analysis and Layer Detection," *Geoscience and Remote Sensing, IEEE Transactions on*, vol. 45, no. 9, pp. 2725–2736, 2007.
- [11] D. M. Schroeder, D. D. Blankenship, and D. A. Young, "Evidence for a water system transition beneath Thwaites Glacier, West Antarctica." *Proceedings of the National Academy of Sciences of the United States of America*, vol. 110, no. 30, pp. 12225–8, Jul. 2013.
- [12] C. Schoof, "Ice-sheet acceleration driven by melt supply variability," *Nature*, vol. 468, no. 7325, pp. 803–806, 2010.
- [13] T. T. Creyts and C. G. Schoof, "Drainage through subglacial water sheets," *Journal of Geophysical Research*, vol. 114, no. F4, p. F04008, Oct. 2009.
- [14] J. S. Walder and A. Fowler, "Channelized subglacial drainage over a deformable bed," *Journal of Glaciology*, vol. 40, no. 134, pp. 3–15, 1994.
- [15] M. Siegert and J. Ridley, "Determining basal ice-sheet conditions in the dome c region of east antarctica using satellite radar altimetry and airborne radio-echo sounding," *Journal of Glaciology*, vol. 44, no. 146, pp. 1–8, 1998.
- [16] A. M. Gades, C. F. Raymond, H. Conway, and R. W. Jacobel, "Bed properties of Siple Dome and adjacent ice streams, West Antarctica, inferred from radio-echo sounding measurements," *Journal of Glaciology*, vol. 46, no. 152, 2000.
- [17] J. A. Dowdeswell and S. Evans, "Investigations of the form and fl w of ice sheets and glaciers using radio-echo sounding," *Reports on Progress in Physics*, vol. 67, no. 10, pp. 1821–1861, Oct. 2004.
- [18] S. P. Carter, D. D. Blankenship, D. A. Young, M. E. Peters, J. W. Holt, and M. J. Siegert, "Dynamic distributed drainage implied by the fl w evolution of the 1996–1998 Adventure Trench subglacial lake discharge," *Earth and Planetary Science Letters*, vol. 283, no. 1–4, pp. 24–37, Jun. 2009.
- [19] J. A. MacGregor, D. P. Winebrenner, H. Conway, K. Matsuoka, P. A. Mayewski, and G. D. Clow, "Modeling englacial radar attenuation at Siple Dome, West Antarctica, using ice chemistry and temperature data," *J. Geophys. Res.*, vol. 112, no. F3, p. F03008, Jul. 2007.
- [20] K. Matsuoka, "Pitfalls in radar diagnosis of ice-sheet bed conditions: Lessons from englacial attenuation models," *Geophys. Res. Lett.*, vol. 38, no. 5, p. L05505, Mar. 2011.
- [21] K. Matsuoka, J. A. MacGregor, and F. Pattyn, "Predicting radar attenuation within the Antarctic ice sheet," *Earth and Planetary Science Letters*, vol. 359–360, no. 0, pp. 173–183, Dec. 2012.
- [22] R. Raney, B. Gotwels, and J. Jensen, "Optimal processing of radar ice sounding data," in *Geoscience and Remote Sensing Symposium, 1999. IGARSS'99 Proceedings. IEEE 1999 International*, vol. 1. IEEE, 1999, pp. 92–94.
- [23] R. Raney, "Radar ice sounder with parallel doppler processing," Feb. 13 2001, US Patent 6,188,348.
- [24] A. A. G. Fountain and J. S. Walder, "Water fl w through temperate glaciers," *Reviews of Geophysics*, vol. 36, no. 3, pp. 299–328, 1998.
- [25] J. W. Holt, D. D. Blankenship, D. L. Morse, D. A. Young, M. E. Peters, S. D. Kempf, T. G. Richter, D. G. Vaughan, and H. F. J. Corr, "New boundary conditions for the West Antarctic Ice Sheet: Subglacial topography of the Thwaites and Smith glacier catchments," *Geophysical Research Letters*, vol. 33, no. 9, p. L09502, May 2006.
- [26] I. R. Joughin, S. Tulaczyk, J. L. Bamber, D. D. Blankenship, J. W. Holt, T. Scambos, and D. G. Vaughan, "Basal conditions for Pine Island and Thwaites Glaciers, West Antarctica, determined using satellite and airborne data," *Journal of Glaciology*, vol. 55, no. 190, pp. 245–257, Apr. 2009.
- [27] A. C. Lough, D. A. Wiens, C. G. Barcheck, S. Anandakrishnan, R. C. Aster, D. D. Blankenship, A. D. Huerta, A. Nyblade, D. A. Young, and T. J. Wilson, "Seismic detection of an active subglacial magmatic complex in marie byrd land, antarctica," *Nature Geoscience*, 2013.
- [28] J. C. Behrendt, D. D. Blankenship, C. A. Finn, R. E. Bell, R. E. Sweeney, S. M. Hodge, and J. M. Brozena, "Casertz aeromagnetic data reveal late cenozoic floo basalts (?) in the west antarctic rift system," *Geology*, vol. 22, no. 6, pp. 527–530, 1994.
- [29] D. D. Blankenship, R. E. Bell, S. M. Hodge, J. M. Brozena, J. C. Behrendt, and C. A. Finn, "Active volcanism beneath the West Antarctic ice sheet and implications for ice-sheet stability," *Nature*, 1993.
- [30] G. Raju and R. K. Moore, "A matched-filte technique for removing hyperbolic effects due to point scatterers: Simulation and application on antarctic radar data," *Geoscience and Remote Sensing, IEEE Transactions on*, vol. 28, no. 4, pp. 726–729, 1990.
- [31] C. Leuschen and R. Plumb, "A matched-filte approach to wave migration," *Journal of applied geophysics*, vol. 43, no. 2, pp. 271–280, 2000.
- [32] J. J. Legarsky, S. P. Gogineni, and T. L. Akins, "Focused synthetic aperture radar processing of ice-sounder data collected over the greenland ice sheet," *Geoscience and Remote Sensing, IEEE Transactions on*, vol. 39, no. 10, pp. 2109–2117, 2001.
- [33] F. Heliere, C. C.-C. Lin, F. Heliere, H. Corr, and D. G. Vaughan, "Radio Echo Sounding of Pine Island Glacier, West Antarctica: Aperture Synthesis Processing and Analysis of Feasibility From Space," *Geoscience and Remote Sensing, IEEE Transactions on*, vol. 45, no. 8, pp. 2573–2582, 2007.
- [34] J. Paden, T. Akins, D. Dunson, C. Allen, and P. Gogineni, "Ice-sheet bed 3-d tomography," *Journal of Glaciology*, vol. 56, no. 195, pp. 3–11, 2010.
- [35] X. Wu, K. C. Jezek, E. Rodriguez, S. Gogineni, F. Rodriguez-Morales, and A. Freeman, "Ice sheet bed mapping with airborne sar tomography," *Geoscience and Remote Sensing, IEEE Transactions on*, vol. 49, no. 10, pp. 3791–3802, 2011.
- [36] C. R. Bentley, D. D. Blankenship, D. G. Schultz, S. T. Rooney, and S. Anandakrishnan, "Geophysical program at upstream b camp, siple coast," *Antarctic Journal of the United States*, vol. 21, no. 5, p. 109, 1986.
- [37] D. G. Schultz, L. A. Powell, and C. R. Bentley, "A digital radar system for echo studies on ice sheets," *Ann. Glaciol.*, vol. 9, pp. 206–210, 1987.
- [38] R. K. Moore, "Modern coherent radar for ice-sheet sounding," *Antarctic Journal of the United States*, vol. 22, no. 5, p. 83, 1987.
- [39] S. Gogineni, T. Chuah, C. Allen, K. Jezek, and R. K. Moore, "An improved coherent radar depth sounder," *Journal of Glaciology*, vol. 44, no. 148, pp. 659–669, 1998.
- [40] A. Moussessian, R. Jordan, E. Rodriguez, A. Safaeinili, T. Akins, W. Edelstein, Y. Kim, and S. Gogineni, "A new coherent radar for ice sounding in greenland," in *Geoscience and Remote Sensing Symposium, 2000. Proceedings. IGARSS 2000. IEEE 2000 International*, vol. 2. IEEE, 2000, pp. 484–486.
- [41] M. E. Peters, D. D. Blankenship, and D. L. Morse, "Analysis techniques for coherent airborne radar sounding: Application to West Antarctic ice streams," *Journal of Geophysical Research*, vol. 110, no. B6, p. B06303, Jun. 2005.
- [42] J. A. MacGregor, G. a. Catania, H. Conway, D. M. Schroeder, I. Joughin, D. A. Young, S. D. Kempf, and D. D. Blankenship, "Weak bed control of the eastern shear margin of Thwaites Glacier, West Antarctica," *Journal of Glaciology*, vol. 59, no. 217, pp. 900–912, 2013.
- [43] S. Nayar, K. Ikeuchi, and T. Kanade, "Surface reflection physical and geometrical perspectives," *IEEE Transactions on Pattern Analysis*, vol. 13, no. 7, pp. 611–634, 1991.
- [44] V. Sarma, N. Prasad, and P. R. Prasad, "The effect of hydrogeology on variations in the electrical conductivity of groundwater fluctuations" *Journal of Hydrology*, vol. 44, no. 1, pp. 81–87, 1979.
- [45] E. F. Knott, J. F. Shaeffer, and M. T. Tuley, *Radar cross section*. Raleigh: SciTech Publishing, 2004.